Isotope-induced elastic scattering of optical phonons in individual suspended single-walled carbon nanotubes

Pei Zhao,[1] Erik Einarsson,[1,2] Rong Xiang,[3] Yoichi Murakami,[4]
Shohei Chiashi,[1] Junichiro Shiomi,[1] and Shigeo Maruyama[1,*]

[1] *Department of Mechanical Engineering, The University of Tokyo, 7-3-1 Hongo, Bunkyo-ku, Tokyo 113-8656, Japan*
[2] *Global Center of Excellence for Mechanical Systems Innovation, The University of Tokyo, 7-3-1 Hongo, Bunkyo-ku, Tokyo 113-8656, Japan*
[3] *State Key Laboratory of Optoelectronic Materials and Technologies, School of Physics and Engineering, Sun Yat-Sen University, Guangzhou 510275, China*
[4] *Global Edge Institute, Tokyo Institute of Technology, 2-12-1 Ookayama, Meguro-ku, Tokyo 152-8550, Japan*

(Dated: August 10, 2011)

Isotope-induced scattering of optical phonons in individual single-walled carbon nanotubes (SWNTs) was investigated by resonance Raman scattering measurements of more than 600 suspended, isotope-mixed SWNTs. The G^+ and G^- features in the SWNT G-band exhibit broadening of up to 80% and 25%, respectively, indicating a reduced lifetime of the corresponding longitudinal and transverse optical (LO & TO) phonons. We propose that this reduced lifetime is due to a combination of enhanced phonon scattering by isotopic inhomogeneity and overbending in the LO phonon branch, both of which increase the scattering rate.

PACS numbers: 61.48.De

The presence of both ^{12}C and ^{13}C in a single-walled carbon nanotube (SWNT) induces mass inhomogeneity while leaving the majority of physical and chemical properties unaltered. This enables phonon-related properties and processes to be better identified and studied. However, most studies on electron-phonon interactions in isotope-mixed SWNTs have been limited to comparing relative Raman peak positions [1, 2]. Turning our attention to lineshapes allows us to investigate phonon physics in more detail, especially concerning the longitudinal and transverse optical (LO & TO) phonons that give rise to the prominent G-band in SWNT Raman spectra.

Here we present a Raman spectroscopy study on the scattering of optical phonons in isotope-mixed SWNTs. Resonance Raman spectra from more than 600 individual suspended SWNTs containing various ^{13}C concentrations show clear broadening of both the G^+ and G^- features in the G-band. We attribute this broadening to an elastic scattering process, which exists in addition to the usual decay of optical phonons into acoustic phonons [3, 4]. We propose that this process is allowed because of so-called 'overbending' of the LO phonon branch near the Γ-point in the Brillouin zone [5], and is enhanced by isotope-induced mass inhomogeneity. These findings are in agreement with a recent study investigating the the influence of ^{13}C concentration on the D and G' (or $2D$) Raman peaks in dispersed SWNT mats [6].

Suspended SWNTs were synthesized on Si/SiO_2 substrates patterned with trenches approximately 4 μm wide and 10 μm deep using the alcohol catalytic CVD method [7]. A cross-sectional scanning electron microscope (SEM) image of the substrate is shown in Fig. 1(a). The sidewalls and bottom of the trenches were coated with 122 nm of Cr in order to deactivate any catalyst and prevent SWNT growth inside the trench. No-flow CVD [8] was performed by introducing a 15 μL mixture containing some concentration β of $^{13}C_2H_5OH$ (Cambridge Isotope Laboratory, Inc.) into a sealed reac-

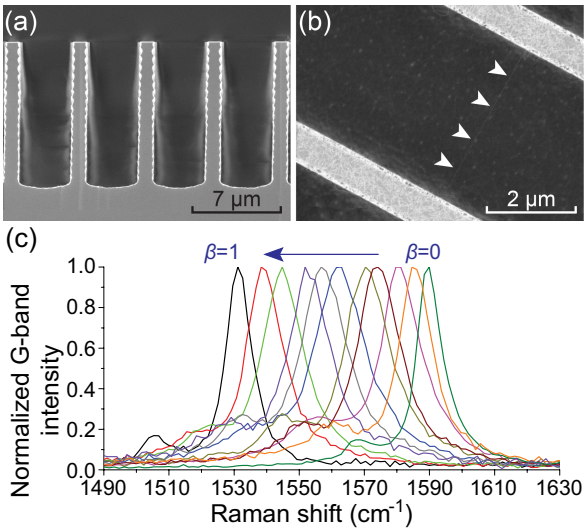

FIG. 1. (a) Cross-sectional SEM image of the patterned substrate before SWNT synthesis and (b) plan view after synthesis. SWNTs were found suspended across the trenches, as indicated by the arrows. (c) Normalized G-band spectra from suspended SWNTs synthesized using ^{13}C carbon concentrations of 0% ($\beta = 0$) to 100% ($\beta = 1$) in 10% increments.

* contact author: maruyama@photon.t.u-tokyo.ac.jp; homepage: www.photon.t.u-tokyo.ac.jp

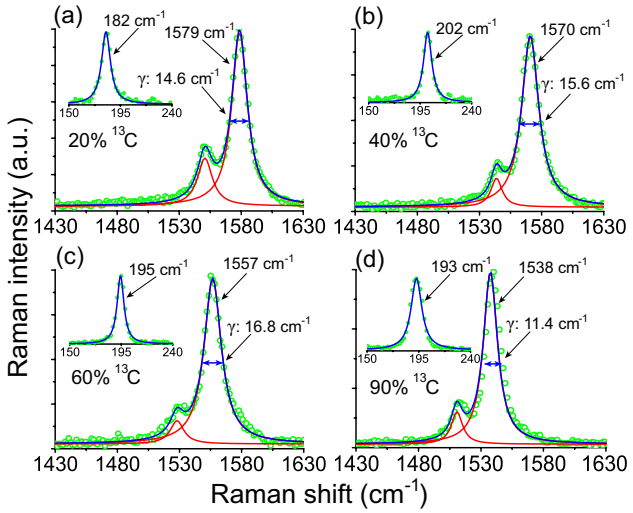

FIG. 2. Resonance Raman spectra (488 nm excitation) from four suspended semiconducting SWNTs with ^{13}C concentrations β of (a) 0.2, (b) 0.4, (c) 0.6, and (d) 0.9. Each G-band was fitted using two Lorentzian lineshapes. Measured data, lineshapes, and fitted curves are shown in green, red and blue, respectively. γ is the FWHM of the G^+ peak, and the inset shows the lone RBM feature observed in each spectrum.

tion chamber. Eleven different concentrations were used, ranging from 0% ($\beta = 0$) to 100% ($\beta = 1$) ^{13}C in 10% increments. Figure 1(b) shows the majority of SWNTs were confined to the narrow regions between the trenches, but some individual SWNTs were found suspended across the trenches (indicated by arrows). Normalized G-band spectra for each concentration are plotted in Fig. 1(c), and clearly show the downshift in G-band frequency expected for increasing ^{13}C concentration [1, 2, 9].

Resonance Raman spectra of the suspended SWNTs were measured in ambient conditions using a 488 nm Ar laser (0.2 mW, 1 μm spot size). We obtained more than 600 resonance Raman spectra that show a clear, *single* RBM peak between 130 cm^{-1} and 210 cm^{-1}, which corresponds to semiconducting SWNTs for 488 nm excitation [10]. Four representative Raman spectra are shown in Fig. 2. The G-band features have been decomposed into their G^+ and G^- components, corresponding to LO and TO phonon modes in semiconducting SWNTs. The peak position and full-width at half-maximum (FWHM) γ of the G^+ feature is shown for each spectrum. Accurate fitting of the G-band using only two Lorentzians, combined with the detection of only a single RBM peak (Fig. 2 inset), suggests that the suspended SWNTs from which these spectra were obtained are either individual or in very small bundles [11].

In addition to downshifts in the Raman peak positions, isotopic inhomogeneity also resulted in significant broadening of both G-band features, as has been observed in bulk nanotube samples [6, 12]. Average γ values for the G^+, G^-, and RBM features for all Raman measurements are shown in Table I. For the G^+ peak, this broadening indicates a considerably shortened LO phonon lifetime (approximately 0.4 ps for β =0.1 and 0.3 ps for β =0.6.) Moreover, this effect appears to have neither diameter nor chirality dependence (not shown), and is determined only by the extent of isotopic inhomogeneity. We note that since electron-phonon coupling does not contribute to TO and LO phonon linewidths in semiconducting SWNTs [13], we consider only phonon-phonon interactions in the following discussion.

TABLE I. Summary of resonance Raman spectral data obtained for isotope-mixed SWNTs, including the number of single-RBM spectra obtained for each ^{13}C concentration (β) and the average FWHM values (γ) of the RBM, G^-, and G^+ features. The excitation laser wavelength was 488 nm.

β	No. of samples	$\gamma_{\rm RBM}$ (cm^{-1})	γ_{G^-} (cm^{-1})	γ_{G^+} (cm^{-1})
0.0	97	8.3	16.7	9.4
0.1	61	8.6	18.7	12.5
0.2	43	8.4	19.8	12.8
0.3	55	8.3	19.9	15.3
0.4	33	8.3	20.1	16.9
0.5	67	8.4	20.7	16.7
0.6	46	8.3	20.1	16.1
0.7	43	8.3	20.0	14.9
0.8	41	8.5	19.7	14.0
0.9	78	8.4	19.0	12.1
1.0	59	8.3	17.1	10.4

The main decay channel for LO phonons is relaxation into acoustic phonons [3, 4]. Mass inhomogeneity is known to induce some additional impurity scattering, but the extent is generally very small (for example, only 1 cm^{-1} for isotope-enriched Si [14].) In diamond, however, isotope-induced scattering is known to be considerably stronger [15]. This has been attributed to a local minimum at the Γ-point, which is known as 'overbending', and can be found in the phonon dispersion relations (p-DOS) of SWNTs [5, 16]. As a result of this overbending, there are degenerate states on the branch into which Γ-point phonons can scatter. Furthermore, the LO and TO branches in SWNTs are separated by an interval distance of tens of cm^{-1} [5], thus elastic scattering of a Γ-point TO phonon into the LO branch is also permitted. This extra scattering process shortens the phonon lifetime, resulting in broadened features in the SWNT Raman spectra.

Using the same model as in [17] for describing the isotope-induced enhancement of phonon collision rate, we describe the linewidths of both G-band features by

$$\gamma = \gamma_{12} + \beta(1-\beta)\gamma_{\rm iso} \; . \qquad (1)$$

γ_{12} is the linewidth for pure ^{12}C-SWNTs, $\gamma_{\rm iso}$ is the broadening contribution due to the presence of isotopes, and β and $(1-\beta)$ are the respective concentrations of ^{13}C and ^{12}C. Since temperature-dependent anharmonic effects are negligible at room temperature [18], any peak broadening induced by the measurement can be neglected. The observed broadening is therefore attributed to

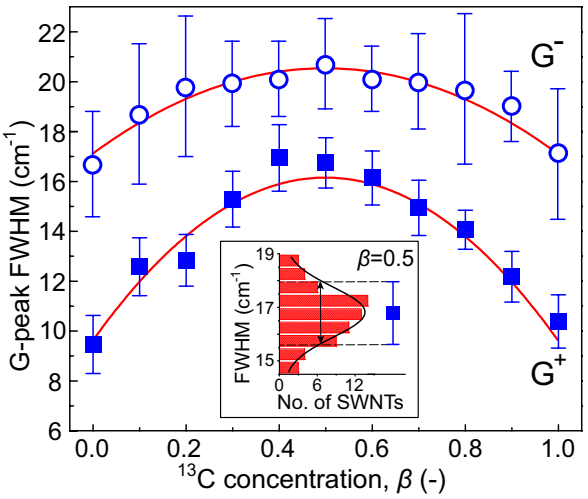

FIG. 3. Average FWHM values of the G^- (open circles) and G^+ (solid squares) Raman peaks in suspended SWNTs as a function of ^{13}C concentration. Red curves are fits of the data using Eq. (1) with $\gamma^-_{12} = 17.1$ cm^{-1} and $\gamma^-_{\rm iso} = 13.6$ cm^{-1} for G^-, and $\gamma^+_{12} = 9.9$ cm^{-1} and $\gamma^+_{\rm iso} = 25.8$ cm^{-1} for G^+ (see text). The inset is a histogram of G^+ FWHM statistics for the case $\beta = 0.5$ showing the symbols indicate statistical average and the bars indicate standard deviation.

the mass inhomogeneity of the SWNTs. The G^+ and G^- data in Table I are plotted in Fig. 3. The red curves are fits to the data using Eq. (1), and the inset shows statistics for the G^+ FWHM for $\beta = 0.5$. The G^+ and G^- FWHM increased by as much as 7 cm^{-1} and 4 cm^{-1}, respectively, which is comparable to the value reported for diamond (~ 5.5 cm^{-1}) in [15].

We note that no broadening was observed for low frequency RBM peaks, although the expected broadening [19] is less than our experimental resolution. We also note that our findings are in good agreement with the very recent report by Costa *et al.* [6], despite different approaches and analysis. Lastly, higher-order anharmonic effects contributing to the broadening of Raman spectral features—as discussed for Si, Ge, and α-Sn by Cardona *et al.* [15]—are not mentioned here because their contributions are negligible in a first-order approximation.

In conclusion, we obtained resonance Raman spectra of more than 600 individual, suspended, isotope-mixed SWNTs. The data show significant broadening of both G^+ and G^- features, and the extent of broadening was dependent on the degree of mass inhomogeneity in the nanotube. The origin of this broadening is attributed to elastic scattering from either the TO or LO branch into the LO branch. This scattering is enhanced by both mass inhomogeneity in the isotope-mixed lattice and overbending in the LO phonon branch near the Γ-point.

ACKNOWLEDGMENTS

Part of this work was financially supported by Grants-in-Aid for Scientific Research (19051016, 19054003 and 22226006) and the Global COE Program 'Global Center for Excellence for Mechanical Systems Innovation'. P.Z. acknowledges a scholarship granted by the China Scholarship Council. The authors thank T.F. Heinz and H.G. Yan at Columbia University, as well as C. Kramberger at the University of Tokyo for helpful discussions.

[1] Y. Q. Cheng, S. Y. Zhou, and B. F. Zhu, Phys. Rev. B **72**, 035410 (2005).
[2] L. Liu and S. S. Fan, J. Am. Chem. Soc. **123**, 11502 (2001).
[3] P. G. Klemens, Phys. Rev. **148**, 845 (1966).
[4] I. Chatzakis, H. Yan, D. Song, S. Berciaud, and T. F. Heinz, Phys. Rev. B **83**, 205411 (2011).
[5] J. Maultzsch, S. Reich, C. Thomsen, E. Dobardžić, I. Milošević, and M. Damnjanović, Solid State Commun. **121**, 471 (2002).
[6] S. D. Costa, C. Fantini, A. Righi, A. Bachmatiuk, M. H. Rümmeli, R. Saito, and M. A. Pimenta, Carbon , in press (2011).
[7] S. Maruyama, R. Kojima, Y. Miyauchi, S. Chiashi, and M. Kohno, Chem. Phys. Lett. **360**, 229 (2002).
[8] R. Xiang, Z. Zhang, K. Ogura, J. Okawa, E. Einarsson, Y. Miyauchi, J. Shiomi, and S. Maruyama, Jpn. J. Appl. Phys. **47**, 1971 (2008).
[9] F. Simon, C. Kramberger, R. Pfeiffer, H. Kuzmany, V. Zólyomi, J. Kürti, P. M. Singer, and H. Alloul, Phys. Rev. Lett. **95**, 017401 (2005).
[10] M. S. Dresselhaus, G. Dresselhaus, R. Saito, and A. Jorio, Phys. Rep. **409**, 47 (2005).
[11] T. Michel, M. Paillet, D. Nakabayashi, M. Picher, V. Jourdain, J. C. Meyer, A. A. Zahab, and J. -L. Sauvajol, Phys. Rev. B **80**, 245416 (2009).
[12] C. Kramberger, M. Löffler, M. Rümmeli, A. Grüneis, R. Schönfelder, O. Jost, T. Gemming, T. Pichler, and B. Büchner, Phys. Status Solidi B **243**, 3050 (2006).
[13] M. Lazzeri, S. Piscanec, F. Marui, A. C. Ferrari, and J. Robertson, Phys. Rev. B **73**, 155426 (2006).
[14] F. Widulle, T. Ruf, M. Konuma, I. Silier, W. Kriegseis, M. Cardona, and V. I. Ozhogin, Solid State Commun. **118**, 1 (2001).
[15] M. Cardona and M. L. W. Thewalt, Rev. Mod. Phys. **77**, 1173 (2005).
[16] J. Koltai, V. Zólyomi, and J. Kürti, Phys. Status Solidi B **245**, 2137 (2008).
[17] S. Maruyama, Y. Igarashi, Y. Taniguchi, and J. Shiomi, J. Therm. Sci. Tech. **1**, 138 (2006).
[18] A. Jorio, C. Fantini, M. S. S. Dantas, M. A. Pimenta, A. G. Souza Filho, Ge. G. Samsonidze, V. W. Brar, G. Dresselhaus, M. S. Dresselhaus, A. K. Swan, M. S. Ünlü, B. B. Goldberg, and R. Saito, Phys. Rev. B **66**, 115411 (2002).
[19] V. Zólyomi, F. Simon, Á. Rusznyák, R. Pfeiffer, H. Peterlik, H. Kuzmany, and J. Kürti, Phys. Rev. B **75**, 195419 (2007).